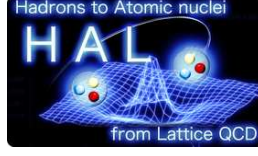


Hyperon forces from lattice quantum chromodynamics at almost physical point: $(m_\pi, m_K) \approx (146, 525)$ MeV/c

H. Nemura¹ and N. Ishii¹



¹Research Center for Nuclear Physics (RCNP), Osaka University, Ibaraki, Osaka 567-0047, Japan

Introduction. The elucidation of the nuclear forces including nucleon-nucleon (NN), hyperon-nucleon (YN) and hyperon-hyperon (YY) from fundamental perspective in terms of quarks and gluons is one of the most important tasks of nuclear physics. For the NN sector, high-precision phenomenological potentials are available to describe the NN scattering data at low energies as well as the deuteron properties. The energy levels of light nuclei are well reproduced by such an NN potential together with a three-nucleon force. On the other hand, phenomenological descriptions of YN and YY interactions are not well constrained from experimental data because of the short life time of hyperons. A recent experimental study shows a tendency to repulsive Σ -nucleus interaction and only a four-body Σ -hypernucleus (${}^4_\Sigma\text{He}$) has been observed; those suggests a repulsive nature of the ΣN interaction. Such quantitative understanding is useful to study properties of hyperonic matter inside the neutron stars, where recent observations of massive neutron star heavier than $2M_\odot$ might raise a problem of hyperonic equation of state (EOS) employed in such a study. Better understanding of YN and YY interactions is becoming increasingly important due to the observation of the binary neutron star merger.

During the last decade a new lattice QCD approach to study a hadron-hadron interaction has been proposed [1, 2], which has been improved to acquire an enhancement in numerical efficiency [3]. In this approach, the interhadron potential is obtained from the lattice QCD measurement of the Nambu-Bethe-Salpeter (NBS) wave function. The observables such as the phase shifts and the binding energies are calculated by using the resultant potential. This approach has been applied to various baryonic interactions [4, 5, 6, 7, 8, 9, 10, 11, 12, 13, 14], and has been extended to systems in inelastic channels [15, 16, 17]. This approach is now called HAL QCD method because almost all the recent developments cited above have been provided by the HAL QCD Collaboration [18].

In the recent few years, the 2+1 flavor lattice QCD calculations have been widely performed to obtain baryon-baryon (BB) potentials. The flavor symmetry breaking is one of the key topics in the study of the isospin symmetric baryon-baryon interactions based on the 2 + 1 flavor lattice QCD. This is an opportune moment to go beyond the BB potentials at the flavor $SU(3)$ point [9] since exploring breakdown of the flavor symmetry is not only an intriguing subject but also a major concern of the phenomenological YN and YY interaction models. In such a situation, it is advantageous to calculate a large number of NBS wave functions of various BB channels simultaneously in a single lattice QCD calculation. For example, we consider the following 52 four-point correlation functions in order to study the complete set of BB interactions in the isospin symmetric limit [19, 20]. (For the moment, we assume that the electromagnetic interaction is not taken into account in the present lattice calculation.)

$$\langle p n \bar{p} \bar{n} \rangle, \tag{1}$$

$$\begin{aligned} &\langle p \Lambda \bar{p} \bar{\Lambda} \rangle, & \langle p \Lambda \bar{\Sigma}^+ \bar{n} \rangle, & \langle p \Lambda \bar{\Sigma}^0 \bar{p} \rangle, \\ &\langle \Sigma^+ n \bar{p} \bar{\Lambda} \rangle, & \langle \Sigma^+ n \bar{\Sigma}^+ \bar{n} \rangle, & \langle \Sigma^+ n \bar{\Sigma}^0 \bar{p} \rangle, \\ &\langle \Sigma^0 p \bar{p} \bar{\Lambda} \rangle, & \langle \Sigma^0 p \bar{\Sigma}^+ \bar{n} \rangle, & \langle \Sigma^0 p \bar{\Sigma}^0 \bar{p} \rangle, \end{aligned} \tag{2}$$

$$\begin{aligned} &\langle \Lambda \Lambda \bar{\Lambda} \bar{\Lambda} \rangle, & \langle \Lambda \Lambda \bar{p} \bar{\Xi}^- \rangle, & \langle \Lambda \Lambda \bar{n} \bar{\Xi}^0 \rangle, & \langle \Lambda \Lambda \bar{\Sigma}^+ \bar{\Sigma}^- \rangle, & \langle \Lambda \Lambda \bar{\Sigma}^0 \bar{\Sigma}^0 \rangle, \\ &\langle p \Xi^- \bar{\Lambda} \bar{\Lambda} \rangle, & \langle p \Xi^- \bar{p} \bar{\Xi}^- \rangle, & \langle p \Xi^- \bar{n} \bar{\Xi}^0 \rangle, & \langle p \Xi^- \bar{\Sigma}^+ \bar{\Sigma}^- \rangle, & \langle p \Xi^- \bar{\Sigma}^0 \bar{\Sigma}^0 \rangle, & \langle p \Xi^- \bar{\Sigma}^0 \bar{\Lambda} \rangle, \\ &\langle n \Xi^0 \bar{\Lambda} \bar{\Lambda} \rangle, & \langle n \Xi^0 \bar{p} \bar{\Xi}^- \rangle, & \langle n \Xi^0 \bar{n} \bar{\Xi}^0 \rangle, & \langle n \Xi^0 \bar{\Sigma}^+ \bar{\Sigma}^- \rangle, & \langle n \Xi^0 \bar{\Sigma}^0 \bar{\Sigma}^0 \rangle, & \langle n \Xi^0 \bar{\Sigma}^0 \bar{\Lambda} \rangle, \\ &\langle \Sigma^+ \Sigma^- \bar{\Lambda} \bar{\Lambda} \rangle, & \langle \Sigma^+ \Sigma^- \bar{p} \bar{\Xi}^- \rangle, & \langle \Sigma^+ \Sigma^- \bar{n} \bar{\Xi}^0 \rangle, & \langle \Sigma^+ \Sigma^- \bar{\Sigma}^+ \bar{\Sigma}^- \rangle, & \langle \Sigma^+ \Sigma^- \bar{\Sigma}^0 \bar{\Sigma}^0 \rangle, & \langle \Sigma^+ \Sigma^- \bar{\Sigma}^0 \bar{\Lambda} \rangle, \\ &\langle \Sigma^0 \Sigma^0 \bar{\Lambda} \bar{\Lambda} \rangle, & \langle \Sigma^0 \Sigma^0 \bar{p} \bar{\Xi}^- \rangle, & \langle \Sigma^0 \Sigma^0 \bar{n} \bar{\Xi}^0 \rangle, & \langle \Sigma^0 \Sigma^0 \bar{\Sigma}^+ \bar{\Sigma}^- \rangle, & \langle \Sigma^0 \Sigma^0 \bar{\Sigma}^0 \bar{\Sigma}^0 \rangle, \\ & & \langle \Sigma^0 \Lambda \bar{p} \bar{\Xi}^- \rangle, & \langle \Sigma^0 \Lambda \bar{n} \bar{\Xi}^0 \rangle, & \langle \Sigma^0 \Lambda \bar{\Sigma}^+ \bar{\Sigma}^- \rangle, & & \langle \Sigma^0 \Lambda \bar{\Sigma}^0 \bar{\Lambda} \rangle, \end{aligned} \tag{3}$$

$$\begin{aligned} &\langle \Xi^- \bar{\Lambda} \bar{\Xi}^- \bar{\Lambda} \rangle, & \langle \Xi^- \bar{\Lambda} \bar{\Sigma}^- \bar{\Xi}^0 \rangle, & \langle \Xi^- \bar{\Lambda} \bar{\Sigma}^0 \bar{\Xi}^- \rangle, \\ &\langle \Sigma^- \bar{\Xi}^0 \bar{\Xi}^- \bar{\Lambda} \rangle, & \langle \Sigma^- \bar{\Xi}^0 \bar{\Sigma}^- \bar{\Xi}^0 \rangle, & \langle \Sigma^- \bar{\Xi}^0 \bar{\Sigma}^0 \bar{\Xi}^- \rangle, \\ &\langle \Sigma^0 \bar{\Xi}^- \bar{\Xi}^- \bar{\Lambda} \rangle, & \langle \Sigma^0 \bar{\Xi}^- \bar{\Sigma}^- \bar{\Xi}^0 \rangle, & \langle \Sigma^0 \bar{\Xi}^- \bar{\Sigma}^0 \bar{\Xi}^- \rangle, \end{aligned} \tag{4}$$

$$\langle \Xi^- \bar{\Xi}^0 \bar{\Xi}^- \bar{\Xi}^0 \rangle. \tag{5}$$

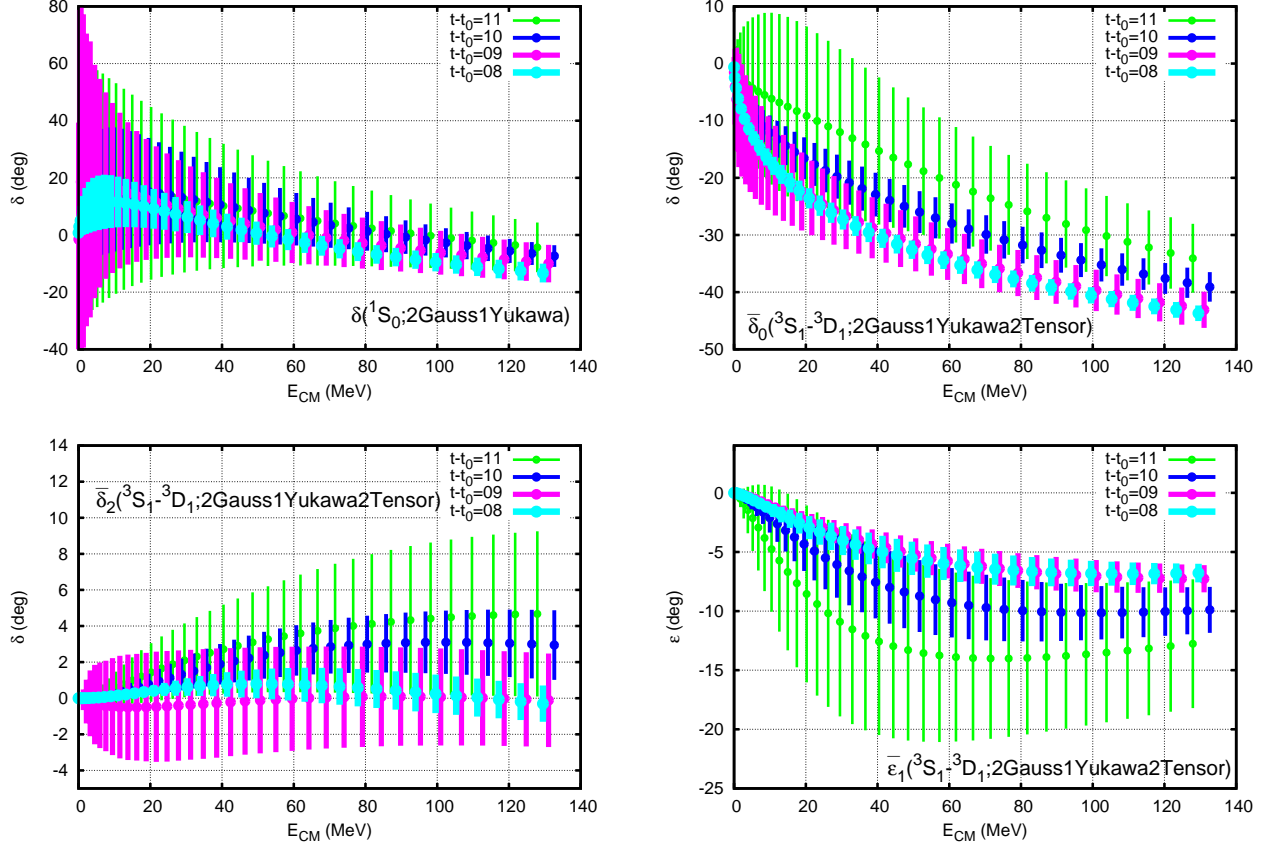


Figure 1: Scattering (bar-)phase shifts and mixing angle of $I = 3/2$ ΣN system, $\delta(^1S_0)$ in the 1S_0 state (upper left), and $\bar{\delta}_0$ (upper right), $\bar{\delta}_2$ (lower left), and $\bar{\varepsilon}_1$ (lower right) in the $^3S_1 - ^3D_1$ states, obtained from the nearly physical point lattice QCD calculation on a volume $(96a)^4 \approx (8.1\text{fm})^4$ with the lattice spacing $a \approx 0.085\text{fm}$ and $(m_\pi, m_K) \approx (146, 525)\text{MeV}$ through parameterized analytical functions. [22]

A large scale lattice QCD calculation [21] is now in progress [22, 23, 24, 25] to study the baryon interactions from NN to $\Xi\Xi$ where a large number of the NBS wave functions are measured simultaneously by using the $2 + 1$ flavor lattice QCD employing directly the almost physical quark masses corresponding to $(m_\pi, m_K) \approx (146, 525)$ MeV and large volume $(La)^4 = (96a)^4 \approx (8.1\text{ fm})^4$ with the lattice spacing $a \approx 0.085\text{fm}$. See also Ref. [26] for the study of $\Omega\Omega$ interaction. The single baryon's masses are measured at the present statistics as $(m_N, m_\Lambda, m_\Sigma, m_\Xi) \approx (962(12), 1139(2), 1221(3), 1354(1))\text{MeV}$, where the number in the parenthesis is the statistical error. The purpose of this report is to present our recent results of hyperon interactions from almost physical point lattice QCD calculation. As one can expect from the Eqs.(1)-(5), so many potentials will be obtained in this study. Classification in terms of irreducible representation (*irrep*) of the flavor $SU(3)$ is very useful to capture consequences of the results. Therefore we restrict ourselves to several particular channels which have relatively simple relationship with *irrep* potentials in the flavor $SU(3)$ limit. In this report, we will show the results of the strangeness $S = -1$ sector and $S = -3$ sector obtained using $2+1$ flavor QCD gauge configurations at almost physical point.

Results of $S = -1$ sector. The result of $S = -1$ sector comprises two parts. One is ΣN single channel with isospin $I = 3/2$ and the other is $\Lambda N - \Sigma N$ coupled-channel with $I = 1/2$. In this report, we concentrate on the scattering phase shifts of $\Sigma N (I = 3/2)$ channel that can be directly compared with other approaches. For detail, see Ref.[22], which includes the other results of the $S = -1$ sector. Figure 1 shows the scattering phase shifts of ΣN system with isospin $I = 3/2$ obtained from the nearly physical point lattice QCD results of the ΣN potentials at Euclidean time slices $t - t_0 = 8 - 11$ after parameterized by analytical functions [22]. Note that, although increasing the imaginary time is favorable in suppressing the uncertainty due to mixing of unwanted excited states, the larger imaginary time causes an increase in statistical error, which raises a serious problem in multi-baryon sector. In this respect, it is very important to emphasize that the HAL QCD method is free from such a problem, since it can positively utilize the “elastic” excited states by using the time-dependent HAL QCD method [3]. If this advantage is dismissed, one has to rely on a tremendously large

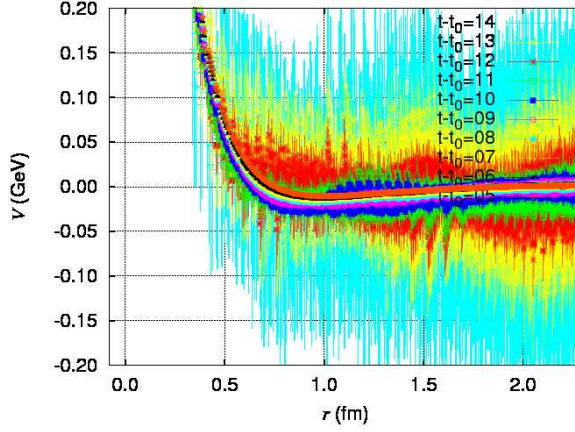


Figure 2: The ΣN central potential of in the $I = 3/2, {}^1S_0$ channel.

amount of imaginary time which requires also a huge amount of electric and CPU power resources. This is the case for naïve Lüscher’s approaches for multi-baryon sector; see Refs. [27, 28, 29] for the details. The upper left panel shows the scattering phase shift in 1S_0 channel; the present result shows that the interaction in the 1S_0 channel is attractive on average. The other three panels in the Figure show the bar-phase shifts and mixing angle in the ${}^3S_1 - {}^3D_1$ states, $\bar{\delta}_0$ (upper right), $\bar{\delta}_2$ (lower left), and $\bar{\varepsilon}_1$ (lower right), respectively; the phase shift $\bar{\delta}_0$ shows the interaction is repulsive while the phase shift $\bar{\delta}_2$ behaves around almost zero degree. The present results are qualitatively consistent with group theoretical classification based on quark model which is useful for clarifying the general behavior of various BB interactions in the S -wave; the ΣN $I = 3/2$ ${}^3S_1 - {}^3D_1$ belongs to $\mathbf{10}$ which is almost Pauli forbidden while the ΣN $I = 3/2$ 1S_0 belongs to $\mathbf{27}$ which is same as NN 1S_0 . The present S -wave (dominated) phase shifts, the repulsive (attractive) behavior of $\bar{\delta}_0$ ($\delta({}^1S_0)$), augur well for future quantitative conclusions with larger statistics. Incidentally, these behaviors are also qualitatively similar to recent studies [30, 31, 32, 33]. The possibility of “mirage” is pointed out [27] for the calculations with larger quark masses for the $\Sigma^- n$ channel that are found in Ref. [30]. The central potential obtained from the ΣN ($I = 3/2, {}^1S_0$) state is shown in Figure 2, which may be compared with the potentials given below ($\Xi\Sigma(I = 3/2)$ and $NN(I = 1)$ in the 1S_0 channel) that relate to $\mathbf{27}$ irrep of the flavor $SU(3)$.

Results of $S = -3$ sector. By following a similar procedure, we obtain the baryon-baryon potential in $S = -3$ sector. The baryon-baryon channels in the $S = -3$ sector consist of two part. One is a single channel sector of $\Xi\Sigma(I = 3/2)$. The other is a coupled channel sector of $\Xi\Lambda - \Xi\Sigma(I = 1/2)$. Here, we restrict ourselves to the $\Xi\Sigma(I = 3/2)$ single channel sector that belongs to the same irreps. of flavor $SU(3)$ as the NN , i.e., the spin-singlet sector belongs to $\mathbf{27}$ irrep. (dineutron channel), whereas the spin-triplet sector belongs $\mathbf{10}^*$ irrep. (deuteron channel). In Fig. 3(left), we show the spin-singlet central potentials of $\Xi\Sigma(I = 3/2)$ single channel sector obtained from the t region $t = 10, \dots, 16$. Since t -dependence is seen to be less significant, we regard that

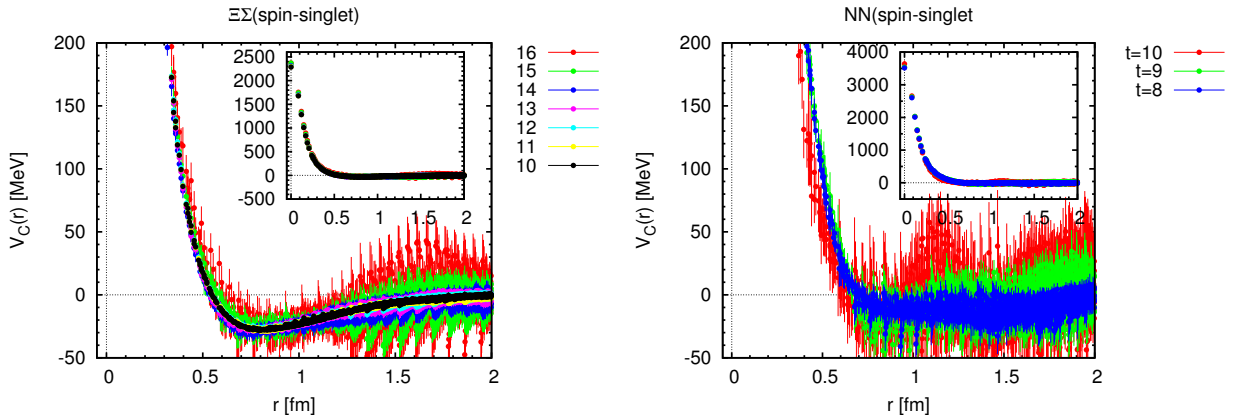


Figure 3: The spin-singlet central potential of $\Xi\Sigma(I = 3/2)$ obtained from t region $t = 10, \dots, 16$ (left) and that of NN obtained from t region $t = 8, 9, 10$ (right) for comparison.

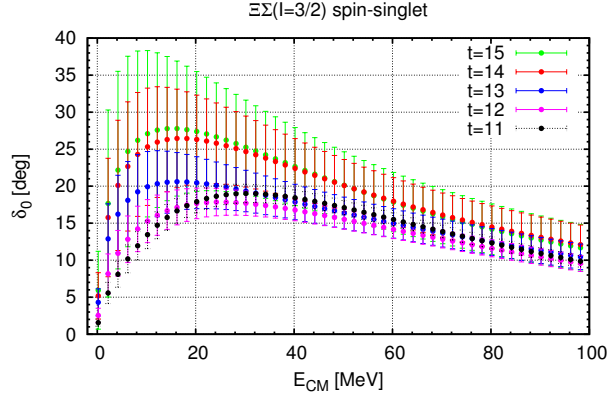


Figure 4: $\Xi\Sigma(I = 3/2)$ scattering phase shift in the spin-singlet sector obtained by solving Schrödinger equation with the $\Xi\Sigma$ potentials in Fig. 3 obtained from t region $t = 11, \dots, 15$.

the potential is converged in this t region. We see that qualitative behaviors are similar to NN, i.e., there is a repulsive core at short distance which is surrounded by attraction. In Fig. 3(right), we show the spin-singlet central potentials of NN($I = 1$) sector obtained from the t region $t = 8, 9, 10$ for comparison. NN potential is seen to have much larger errorbar than $\Xi\Sigma$ potential. This is because NN contains no valence strange quarks whereas $\Xi\Sigma$ contains three valence strange quarks. We compare these two potential to see the size of flavor SU(3) breaking. We see that the strength of the repulsive core is weaker for the $\Xi\Sigma$ potential than NN potential. As for the strength of the attraction, NN is too noisy to conclude anything. Note that the spin singlet sector of $\Sigma N(I = 3/2)$ also belongs to irrep. **27** in the flavor SU(3) limit. Its potential and the phase shift are given in Fig.2 and Fig.1(upper left).

We use the $\Xi\Sigma$ potential to solve Schrödinger equation to obtain the scattering phase shift. The result is shown in Fig. 4. The qualitative behavior is similar to NN, i.e., the $\Xi\Sigma(I = 3/2)$ interaction is attractive, which is not strong enough to generate a bound state.

In Fig. 5 (left) and Fig. 6 (left), we show the spin-triplet central and tensor potentials of $\Xi\Sigma(I = 3/2)$ single channel sector obtained from t region $t = 10, \dots, 16$, respectively. We see that their qualitative behaviors are similar to those of NN. In Fig. 5 (right) and Fig. 6 (right), we show the spin-triplet central and tensor potentials of NN($I = 0$) sector obtained from t region $t = 8, 9, 10$ for comparison. By comparing $\Xi\Sigma(I = 3/2)$ and NN($I = 0$), we see that the repulsive core is weaker for the $\Xi\Sigma$ than NN and that the strength of the tensor force is weaker for the $\Xi\Sigma$ than NN. As for the attraction of the central potential, NN is too noisy to say anything.

We use these $\Xi\Sigma$ potentials to solve Schrödinger equation. The resulting phase shifts are shown in Fig. 7. The qualitative behaviors are similar to NN, i.e., $\Xi\Sigma(I = 3/2)$ interaction in the spin-triplet sector is attractive,

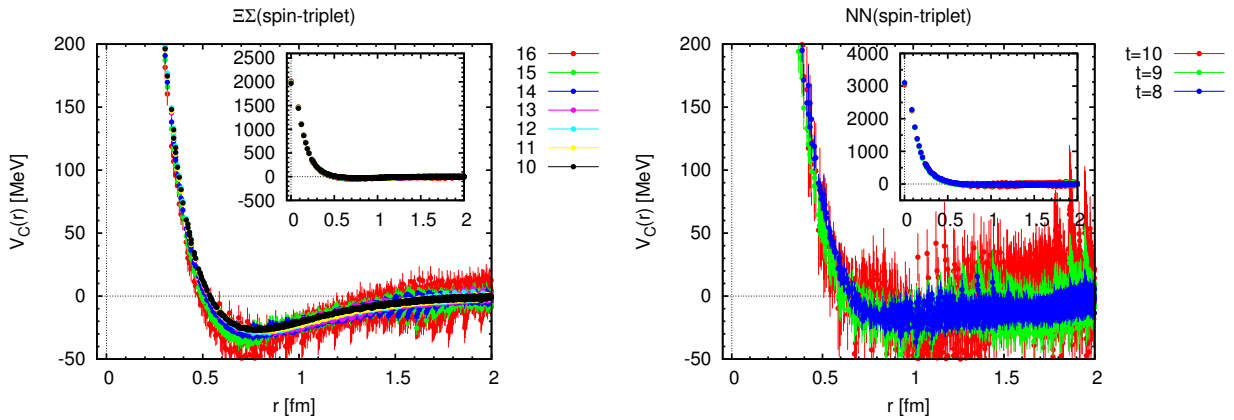


Figure 5: The spin-triplet central potential of $\Xi\Sigma(I = 3/2)$ obtained from t region $t = 10, \dots, 16$ (left) and that of NN obtained from t region $t = 8, 9, 10$ (right).

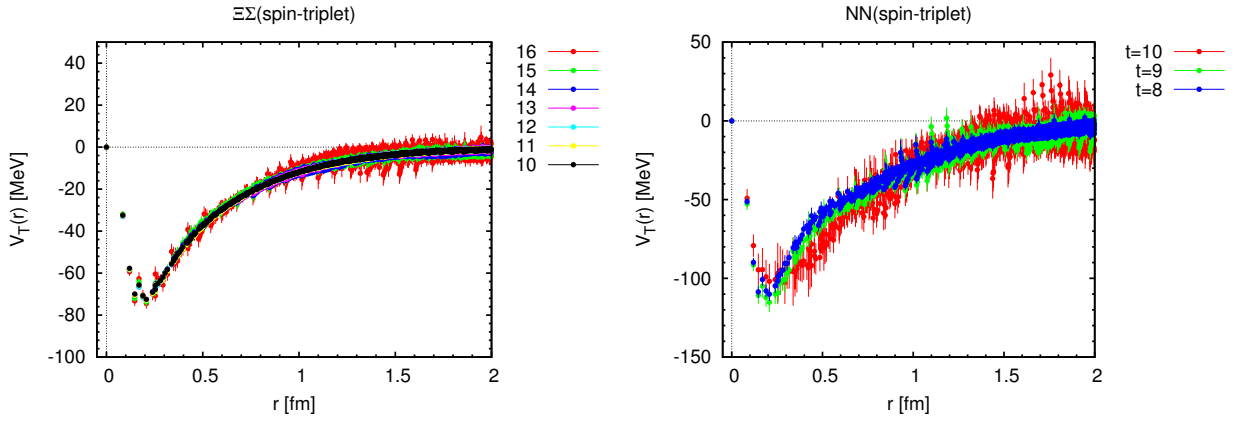


Figure 6: The spin-triplet tensor potential of $\Xi\Sigma(I = 3/2)$ obtained from t region $t = 10, \dots, 16$ (left) and that of NN obtained from t region $t = 8, 9, 10$ (right).

however, the strength is weaker than NN which results in the absence of a bound state.

Summary. In this report, the results of both ΣN with $I = 3/2$ and $\Xi\Sigma$ with $I = 3/2$ interactions are presented by using the 2+1 flavor gauge configurations at almost the physical point. For the ΣN ($I = 3/2$) interaction, phase shifts are calculated for the ${}^3S_1 - {}^3D_1$ and 1S_0 states. The phase shift $\bar{\delta}_0$ in the ${}^3S_1 - {}^3D_1$ channel shows that the ΣN ($I = 3/2, {}^3S_1$) interaction is repulsive. The phase shift in the ΣN ($I = 3/2, {}^1S_0$) channel shows that the interaction is attractive on average. These results are qualitatively consistent with recent phenomenological approaches. For $S = -3$ sector, the $\Xi\Sigma$ ($I = 3/2$) potentials and resulting phase shifts are presented. Interestingly, the 1S_0 (${}^3S_1 - {}^3D_1$) channel of the $\Xi\Sigma$ ($I = 3/2$) belongs to $\mathbf{27}(\overline{\mathbf{10}})$ flavor $SU(3)$ *irrep*, which is same as the 1S_0 (${}^3S_1 - {}^3D_1$) channel of the NN . Therefore NN potentials are also shown for the comparison. Further calculations to obtain physical quantities with increased statistics are in progress and will be reported elsewhere.

References

- [1] N. Ishii, S. Aoki, T. Hatsuda, Phys. Rev. Lett. **99**, 022001 (2007), nucl-th/0611096
- [2] S. Aoki, T. Hatsuda, N. Ishii, Prog. Theor. Phys. **123**, 89 (2010), 0909.5585
- [3] N. Ishii, S. Aoki, T. Doi, T. Hatsuda, Y. Ikeda, T. Inoue, K. Murano, H. Nemura, K. Sasaki (HAL QCD), Phys. Lett. **B712**, 437 (2012), 1203.3642
- [4] K. Murano, N. Ishii, S. Aoki and T. Hatsuda, Prog. Theor. Phys. **125**, 1225 (2011) doi:10.1143/PTP.125.1225 [arXiv:1103.0619 [hep-lat]].
- [5] H. Nemura, N. Ishii, S. Aoki and T. Hatsuda, Phys. Lett. B **673**, 136 (2009) doi:10.1016/j.physletb.2009.02.003 [arXiv:0806.1094 [nucl-th]].
- [6] T. Inoue *et al.* [HAL QCD Collaboration], Prog. Theor. Phys. **124**, 591 (2010) doi:10.1143/PTP.124.591 [arXiv:1007.3559 [hep-lat]].
- [7] T. Inoue *et al.* [HAL QCD Collaboration], Phys. Rev. Lett. **106**, 162002 (2011) doi:10.1103/PhysRevLett.106.162002 [arXiv:1012.5928 [hep-lat]].
- [8] T. Doi *et al.* [HAL QCD Collaboration], Prog. Theor. Phys. **127**, 723 (2012) [arXiv:1106.2276 [hep-lat]].
- [9] T. Inoue *et al.* [HAL QCD Collaboration], Nucl. Phys. A **881**, 28 (2012) [arXiv:1112.5926 [hep-lat]].
- [10] T. Inoue *et al.* [HAL QCD Collaboration], Phys. Rev. Lett. **111**, 112503 (2013) [arXiv:1307.0299 [hep-lat]].
- [11] K. Murano *et al.* [HAL QCD Collaboration], Phys. Lett. B **735**, 19 (2014) [arXiv:1305.2293 [hep-lat]].
- [12] F. Etminan *et al.* [HAL QCD Collaboration], Nucl. Phys. A **928**, 89 (2014) [arXiv:1403.7284 [hep-lat]].
- [13] T. Inoue *et al.* [HAL QCD Collaboration], Phys. Rev. C **91**, no. 1, 011001 (2015) [arXiv:1408.4892 [hep-lat]].

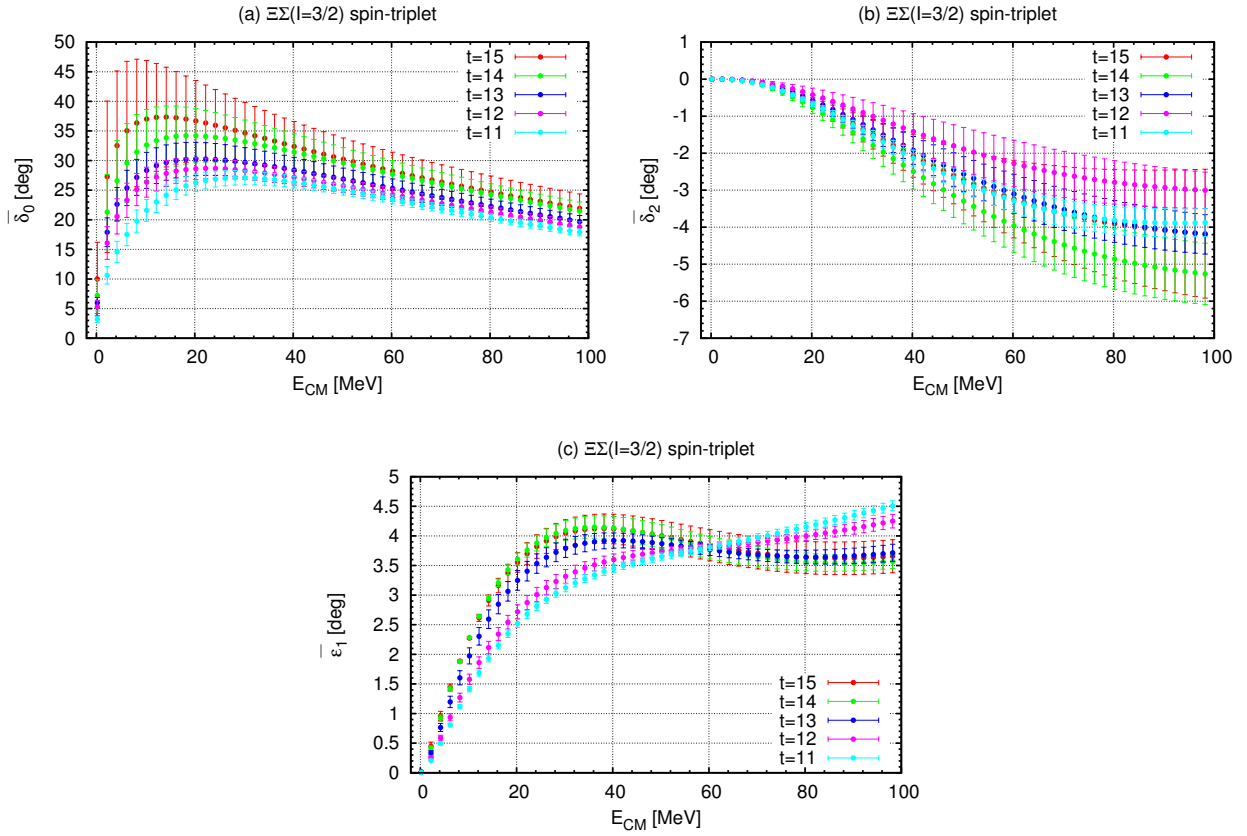


Figure 7: $\Xi\Sigma(I = 3/2)$ scattering phase shift obtained by solving Schrödinger equation with the $\Xi\Sigma$ potentials in Fig. 5 and Fig. 6 obtained from $t = 11, \dots, 15$. (a) s-wave phase shift $\bar{\delta}_0$, (b) d-wave phase shift $\bar{\delta}_2$ and (c) mixing parameter $\bar{\epsilon}_1$.

- [14] M. Yamada *et al.* [HAL QCD Collaboration], PTEP **2015**, no. 7, 071B01 (2015) [arXiv:1503.03189 [hep-lat]].
- [15] S. Aoki *et al.* [HAL QCD Collaboration], Proc. Jpn. Acad. B **87**, 509 (2011) [arXiv:1106.2281 [hep-lat]].
- [16] S. Aoki, B. Charron, T. Doi, T. Hatsuda, T. Inoue and N. Ishii, Phys. Rev. D **87**, no. 3, 034512 (2013) [arXiv:1212.4896 [hep-lat]].
- [17] K. Sasaki *et al.* [HAL QCD Collaboration], PTEP **2015**, no. 11, 113B01 (2015) doi:10.1093/ptep/ptv144 [arXiv:1504.01717 [hep-lat]].
- [18] S. Aoki, T. Doi, T. Hatsuda, Y. Ikeda, T. Inoue, N. Ishii, K. Murano, H. Nemura, K. Sasaki (HAL QCD), PTEP **2012**, 01A105 (2012), 1206.5088
- [19] H. Nemura (HAL QCD), PoS LATTICE2013, 426 (2014)
- [20] H. Nemura, Comput. Phys. Commun. **207**, 91 (2016), 1510.00903
- [21] K.I. Ishikawa, N. Ishizuka, Y. Kuramashi, Y. Nakamura, Y. Namekawa, Y. Taniguchi, N. Ukita, T. Yamazaki, T. Yoshie (PACS), PoS LATTICE2015, 075 (2016), 1511.09222
- [22] H. Nemura *et al.*, EPJ Web Conf. **175**, 05030 (2018) doi:10.1051/epjconf/201817505030 [arXiv:1711.07003 [hep-lat]].
- [23] N. Ishii *et al.*, EPJ Web Conf. **175**, 05013 (2018). doi:10.1051/epjconf/201817505013
- [24] T. Doi *et al.*, EPJ Web Conf. **175**, 05009 (2018) doi:10.1051/epjconf/201817505009 [arXiv:1711.01952 [hep-lat]].
- [25] K. Sasaki *et al.*, EPJ Web Conf. **175**, 05010 (2018). doi:10.1051/epjconf/201817505010

- [26] S. Gongyo et al. (2017), 1709.00654
- [27] T. Iritani et al., JHEP **10**, 101 (2016), 1607.06371
- [28] T. Iritani [LATTICE-HALQCD Collaboration], EPJ Web Conf. **175**, 05008 (2018) doi:10.1051/epjconf/201817505008 [arXiv:1710.06147 [hep-lat]].
- [29] S. Aoki, T. Doi and T. Iritani, EPJ Web Conf. **175**, 05006 (2018) doi:10.1051/epjconf/201817505006 [arXiv:1707.08800 [hep-lat]].
- [30] S.R. Beane, E. Chang, S.D. Cohen, W. Detmold, H.W. Lin, T.C. Luu, K. Orginos, A. Parreno, M.J. Savage, A. Walker-Loud, Phys. Rev. Lett. **109**, 172001 (2012), 1204.3606
- [31] Y. Fujiwara, C. Nakamoto, Y. Suzuki, Phys. Rev. **C54**, 2180 (1996)
- [32] I. Arisaka, K. Nakagawa, S. Shinmura, M. Wada, Prog. Theor. Phys. **104**, 995 (2000), [Erratum: Prog. Theor. Phys.107,237(2002)]
- [33] J. Haidenbauer, S. Petschauer, N. Kaiser, U.G. Meissner, A. Nogga, W. Weise, Nucl. Phys. **A915**, 24 (2013), 1304.5339